Resistive Instabilities in a Hall Thruster Under the Presence of Collisions and Thermal Motion of Electrons

Sukhmander Singh and Hitendra K. Malik[*]

Plasma Waves and Particle Acceleration Laboratory, Department of Physics, Indian Institute of Technology Delhi, New Delhi – 110 016, India

Abstract: The electrostatic and electromagnetic low frequency waves propagating in azimuthal direction in a Hall thruster channel are found to be unstable due to the resistive coupling to the electrons' closed drift in the presence of collisions. The thermal motion of the electrons and their collisions significantly affect the growth of these waves. With respect to the collision frequency, wave number, electron temperature and plasma density, both the instabilities grow in a similar fashion but they behave oppositely under the effects of magnetic field and electron drift velocity. In both the cases, smaller wavelength oscillations are found to be most unstable, and magnitude of the growth rate of the electrostatic wave supersedes that of the electromagnetic wave. The electrostatic instability is more sensitive to the electron collisions in comparison with the electromagnetic instability. On the other hand, the electromagnetic instability is suppressed in the presence of larger ion drift velocity.

1. INTRODUCTION

Hall thrusters have emerged as an integral part of propulsion technology. Unlike chemicals and electric rockets, in a Hall thruster, the propulsion thrust is achieved by a propellant (usaully Xenon), which is ionized and then acceleated by electrostatic forces. These are versatile electric propulsion devices, where thrust efficiencies can exceed 50% and specific impulses are typically between 20 min and 1 hr. It is interesting that these thrusters adjust their thrust and impulse by varying the acceleration voltage and the flow rate of the propellant. This capability makes them potential candidates for space missions with regard to the spacecraft station keeping, rephrasing and orbit topping applications or the situations where different types of maneuvers require different level of thrust and specific impulse [1-5].

The schematic diagram of a typical Hall plasma thruster is given in Fig. (**1**). It consists of an axis symmetric and annular discharge chamber with an interior metallic anode. A cathode is mounted externally, which produces electrons outside the discharge channel. Generally Xenon gas is injected at the anode as a propellant, which enters the discharge chamber at low velocity. The positively charged anode inside the thruster and the negatively charged electron cloud outside the channel establishes an axial electric field of strength $\sim 10^4$ V/m. By using magnets around the annular channel and along the thruster centerline, a radial magnetic field of moderate strength (~150 – 200G) is created, which is strong enough so that the electrons get magnetized, i.e. they are able to gyrate within the discharge channel, but the ions remain unaffected due to their Larmor radius much larger than the dimension of the thruster. Thus the electrons remain effectively trapped in azimuthally $\vec{E} \times \vec{B}$ drifts around the annular channel and slowly diffuse towards the anode. This azimuthal drift current of the electrons is referred to as the Hall current. These trapped electrons promote ionization by increasing collisionality. Also they transmit thrust to the thruster body through a magnetic pressure force exerted on the magnets. Not only this, the electrons generating at the cathode play an important role in keeping the plume downstream of the thruster quasineutral, otherwise the ions accelerated out of the thruster can cause hazardous spacecraft charging.
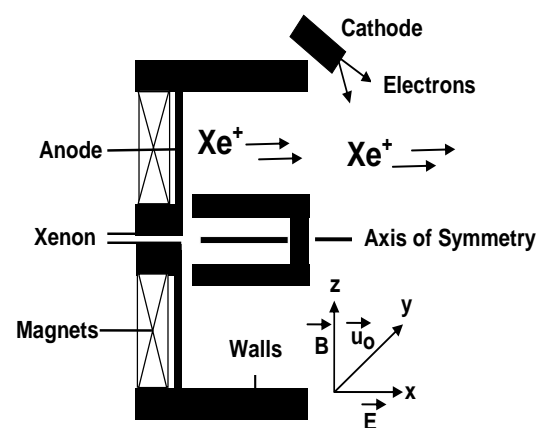
Fig. (1). Schematic diagram of a typical Hall plasma thruster.

*Address correspondence to this author at the Plasma Waves and Particle Acceleration Laboratory, Department of Physics, Indian Institute of Technology Delhi, New Delhi – 110 016, India;
Tel: +91-11-2659-1303; Fax: +91-11-2658-2037;
E-mails: hkmalik@physics.iitd.ac.in, hkmalik@hotmail.com

Two types of Hall thrusters have been developed, which can be categorized into two general groups namely magnetic layer type and anode layer type [6, 7]. The magnetic layer type thruster is the Stationary Plasma Thruster (SPT), which was developed in Russia [8]. In such thrusters, the wall is made up of dielectric such as boron nitride or silicon carbide. In addition the length of their acceleration channel is kept greater than the channel width [9]. The electron temperature in such thrusters is generally low and hence a smooth and continuous variation in the plasma potential between the anode and cathode is obtained. On the other hand, the Thruster with Anode Layer (TAL), also developed in Russia [10, 11], has a narrow acceleration zone. This reduces the loss caused by ion and electron collisions with the walls. The walls of such thrusters are made up of conductor. Since the walls are conductive, a constant potential (same as that of the cathode) is observed along the entire wall. Very high electron temperatures (more than 50 eV) are typically observed in such thrusters.

In order to improve the performance of the Hall thruster, we need to understand the inner physical phenomena such as the instability of the discharge current and plasma oscillations that play an important role in controlling the transport, conduction and mobility in these devices. Different types of the discharge instabilities with frequencies ranging from kHz to GHz have been reported in Hall thruster [12]. Litvak and Fisch [13] have investigated resistive instabilities in a Hall current plasma discharge and found that plasma perturbations in the acceleration channel are unstable in the presence of collisions. Fernandez *et al.* [14] did simulations for the growth of resistive instability. Keidar [15] has modeled plasma dynamics and ionization of propellant gas within the anode holes used for gas injection of a Hall thruster. He along with Beilis [16] obtained the sheath and boundary conditions for plasma simulations of a Hall thruster discharge with magnetic lenses. Keidar and Boyd [17] have studied the effect of magnetic field on the plasma plume. Litvak and Fisch [18] have analyzed gradient driven Rayleigh type instabilities in a Hall thruster using two fluid hydrodynamic equations. Ducrocq *et al.* [19] have investigated high frequency electron drift instability in the cross field configuration of a Hall thruster together with the effect of distorted electron distribution functions obtained in particle-in-cell simulations. Barral and Ahedo [20] have developed a low frequency model of breathing oscillations in Hall discharges, where they observed that unstable modes are strongly nonlinear and are characterized by frequencies obeying a scaling law different from that of linear modes. Boeuf and Garrigues [21] have developed a simple 1D transient, quasineutral hybrid model of a stationary plasma thruster, based on which they had estimated the plasma properties and found them qualitatively close to the experimental observations. Chesta *et al.* [22] have theoretically obtained the growth rate and frequencies of predominantly axial and azimuthally propagating plasma disturbances. Through numerical simulations, they identified the persistence of a low frequency instability associated with the ionization process.

It can be seen that in most of the studies either the temperature of plasma species or the electron collisions have been neglected for the sake of simplicity, though the efficiency and performance of the thrusters are drastically changed by these parameters. Therefore, in order to realize the exact behaviour and the consequences of finite temperature on the thruster efficiency, it is of much importance to investigate the plasma disturbances in Hall thrusters by including the finite temperatures of the plasma species. Under this situation, purely azimuthal electrostatic and electromagnetic waves are found to be unstable due to the resistive coupling to the electrons' $\vec{E} \times \vec{B}$ flow in the presence of electron collisions. Hence, in the present article, we have analytically investigated these resistive instabilities in a Hall thruster in more realistic situation by including the contribution of the pressure gradient force and the collisions of the electrons.

2. PLASMA MODEL AND BASIC EQUATIONS

A Hall thruster with two-component plasma consisting of ions and electrons is considered in which only the electrons are magnetized and the ions are not. The appropriate coordinate system for investigating the waves and instabilities in such a Hall thruster is cylindrical coordinate system. However, consistent to Choueiri [12], Ducrocq *et al.* [19] and Barral and Ahedo [20] we use Cartesian coordinate system for simplification and take the x- axis along the axis of the thruster, i.e. along the applied electric field E_x, and the z- axis along the radius of the thruster in which direction the magnetic field $\vec{B}_0$ $\left(\equiv B_0 \hat{z} \right)$ is applied. The y- axis corresponds to the azimuthal direction. With regard to various parameters, we take n_i (M) as the ion density (mass), $\vec{v}_i$ as the ion fluid velocity, $\vec{E}$ as the electric field, $\vec{B}$ as the magnetic field, n_e (m) as the electron density (mass), $\vec{v}_e$ as the electron fluid velocity, v as the collision momentum transfer frequency between the electrons and neutral atoms. Under this situation, the basic fluid equations for the ion and electron fluids are written as

$$\frac{\partial n_i}{\partial t} + \vec{\nabla} \cdot (\vec{v}_i n_i) = 0 \tag{1}$$

$$M n_i \left[\frac{\partial \vec{v}_i}{\partial t} + (\vec{v}_i \cdot \vec{\nabla}) \vec{v}_i \right] - e n_i \vec{E} = 0 \tag{2}$$

$$\frac{\partial n_e}{\partial t} + \vec{\nabla} \cdot (\vec{v}_e n_e) = 0 \tag{3}$$

$$m n_e \left[\frac{\partial \vec{v}_e}{\partial t} + (\vec{v}_e \cdot \vec{\nabla}) \vec{v}_e \right] + e n_e (\vec{E} + \vec{v}_e \times \vec{B}) + n_e m v \vec{v}_e + \vec{\nabla} p_e = 0 \tag{4}$$

We consider the perturbations to be potential and nondissipative, and take the perturbed densities as n_i and n_e, and velocities as $\vec{v}_i$ and $\vec{v}_e$ along with their unperturbed values as v_0 and u_0, in the x- and y-directions, respectively. The unperturbed density is taken as n_0, electric field (magnetic field) as E_0 (B_0) and the perturbed value of the electric field (magnetic field) is taken as $\vec{E}_1$ ($\vec{B}_1$). In view of small variations of both the density and magnetic field along the channel, the plasma inhomogeneities are neglected. The

perturbations of the ion and electron densities are taken small enough $(n_i, n_e \ll n_0)$ so that the collisional effect due to the velocity perturbations dominate over the one due to the density perturbation, and also the force $en_1 E_0$ can be neglected in comparison with $en_0 E_1$. The linearized form of the above equations thus read

$$\frac{\partial n_i}{\partial t} + \upsilon_0 \frac{\partial n_i}{\partial x} + n_0 (\vec{\nabla} \cdot \vec{\upsilon}_i) = 0 \tag{5}$$

$$M\left(\frac{\partial \vec{\upsilon}_i}{\partial t} + \upsilon_0 \frac{\partial \vec{\upsilon}_i}{\partial x}\right) - e\vec{E}_1 = 0 \tag{6}$$

$$\frac{\partial n_e}{\partial t} + u_0 \frac{\partial n_e}{\partial y} + n_0 (\vec{\nabla} \cdot \vec{\upsilon}_e) = 0 \tag{7}$$

$$m\left[\frac{\partial \vec{\upsilon}_e}{\partial t} + u_0 \frac{\partial \vec{\upsilon}_e}{\partial y}\right] + e(\vec{E}_1 + \vec{\upsilon}_e \times \vec{B}_0 + \vec{u}_0 \times \vec{B}_1) + mv\vec{\upsilon}_e + \frac{\vec{\nabla} p_e}{n_0} = 0 \tag{8}$$

The initial drifts υ_0 and u_0 of the ions and electrons in the channel are related to the electric and magnetic fields according to $\upsilon_0 \dfrac{\partial \upsilon_0}{\partial x} = \dfrac{eE_0}{M}$ and $u_0 = -\dfrac{E_0}{B_0}$ obtained from the unperturbed part of Eqs. (2) and (4). The electron pressure in Eqs. (4) and (8) is given by $p_e = Y_e n_e T_e$ together with T_e as the electron temperature, which we consider to be constant, and Y_e as the ratio of specific heats.

We seek the solution of the above equations, for which the perturbed quantities are taken as $f_1 \sim \exp(i\omega t - ik_x x - ik_y y)$. Here $f_1 \equiv n_i$, n_e, $\vec{\upsilon}_i$, $\vec{\upsilon}_e$, $\vec{E}_1$, $\vec{B}_1$ together with ω as the frequency of oscillations and $\vec{k}$ as the propagation vector. In the next sections, we will derive the dispersion equations for the electrostatic (ES) and electromagnetic (EM) waves, based on which we will estimate the growths of both the waves.

3. ES WAVES: DISPERSION EQUATION AND GROWTH RATE

For the electrostatic disturbances, $\vec{u}_0 \times \vec{B}_1 = 0$ is taken in Eq. (8) and the oscillating electric field is written as $\vec{E}_1 = -\vec{\nabla}\varphi$ together with φ as the perturbed electric potential. With the help of these, the following expressions for the perturbed ion and electron densities are obtained from Eqs. (5 – 8).

$$n_i = \frac{ek^2 n_0}{M(\omega - k_x \upsilon_0)^2} \varphi \tag{9}$$

where $k^2 = k_x^2 + k_y^2$.

$$n_e = \frac{n_0}{(\omega - k_y u_0)}(k_x \upsilon_x + k_y \upsilon_y) \tag{10}$$

The expression for the electron density n_e contains the velocity components υ_x and υ_y, which are derived in terms

of the potential φ under the assumption $\Omega \gg \omega$, $k_y u_0$ and v in view of the oscillations observed in Hall thrusters [13, 22, 23]. Further, taking $\omega - k_y u_0 - iv \equiv \hat{\omega}$, $\dfrac{eB_0}{m} \equiv \Omega$,

$\sqrt{\dfrac{Y_e T_e}{m}} \equiv V_{th}$, $\sqrt{\dfrac{n_0 e^2}{m\varepsilon_0}} \equiv \omega_e$ and $\sqrt{\dfrac{n_0 e^2}{M\varepsilon_0}} \equiv \omega_i$, the expression for n_e is obtained as

$$n_e = \frac{en_0 \hat{\omega}\left[(\Omega^2 + \hat{\omega}^2)\Omega k^2 - ik_x k_y \hat{\omega}^3\right]\varphi}{m\Omega\left[\Omega^4(\omega - k_y u_0) + V_{th}^2(\hat{\omega}k^2 + ik_x k_y)(\Omega^2 + \hat{\omega}^2)\right]} \tag{11}$$

In view of waves propagating purely in azimuthal direction in a real thruster, we put $k_x = 0$ and obtain the following from the Poisson's equation $-k_y^2 \varphi = \dfrac{e(n_e - n_i)}{\varepsilon_0}$ with the help of Eqs. (9) and (11)

$$k_y^2 \varphi + \frac{k_y^2 \omega_e^2 \hat{\omega}(\Omega^2 + \hat{\omega}^2)}{\Omega^4(\omega - k_y u_0) + \hat{\omega}k_y^2 V_{th}^2(\Omega^2 + \hat{\omega}^2)}\varphi - \frac{\omega_i^2 k_y^2 \varphi}{\omega^2} = 0 \tag{12}$$

The above equation after simplification yields

$$\omega^2 \omega_e^2 \hat{\omega}(\Omega^2 + \hat{\omega}^2) + (\omega^2 - \omega_i^2)$$
$$\left[\Omega^4(\omega - k_y u_0) + \hat{\omega}k_y^2 V_{th}^2(\Omega^2 + \hat{\omega}^2)\right] = 0 \tag{13}$$

This is the dispersion equation for the ES waves, showing the effect of finite thermal motion of the electrons, collision frequency, magnetic field, electron drift velocity, azimuthal wave number and ion drift velocity. In order to check the authenticity of this equation, we put $T_e = 0$ and note that this equation reduces to the equation obtained by Litvak and Fisch [13]. In order to find the roots of the above equation, we first solve this for ω and obtain

$$(\omega_e^2 + k_y^2 V_{th}^2)\omega^5 - 3k_y u_0(\omega_e^2 + k_y^2 V_{th}^2)\omega^4$$
$$+\left[\begin{array}{l}(3k_y^2 u_0^2 - 3v^2 + \Omega^2)(\omega_e^2 - k_y^2 V_{th}^2)\\ +\Omega^4 - \omega_i^2 k_y^2 V_{th}^2\end{array}\right]\omega^3$$
$$+\left[\begin{array}{l}k_y u_0(3v^2 - k_y^2 u_0^2 - \Omega^2)(\omega_e^2 - k_y^2 V_{th}^2)\\ -k_y u_0 \Omega^4 + 3k_y^3 u_0 V_{th}^2 \omega_i^2\end{array}\right]\omega^2$$
$$-\left[(3k_y^2 u_0^2 - 3v^2 + \Omega^2)\omega_i^2 k_y^2 V_{th}^2 + \omega_i^2 \Omega^4\right]\omega$$
$$-k_y^3 u_0(3v^2 - k_y^2 u_0^2 - \Omega^2)\omega_i^2 V_{th}^2 + \omega_i^2 \Omega^4 k_y u_0 = 0 \tag{14}$$

Since it is not possible to find an analytical solution of the above equation, we look for the numerical solution along with typical values of B_0, n_0, T_e, u_0, k_y, v and υ_0. In Hall plasma thrusters, these parameters can have the values as thruster channel diameter = 4 – 10 cm, $B_0 = 100 - 200$ G, $n_0 = 5 \times 10^{17} - 10^{18}$ /m^3, $T_e = 10 - 15$ eV, $u_0 \sim 10^6$ m/s, $v \sim 10^6$ /s and $\upsilon_0 = 2 \times 10^4 - 5 \times 10^4$ m/s [21-23]. With regard to the value of k_y, we constraint $k_y = -\dfrac{m}{r}$ (where r is the radius of thruster channel) together with $m = 1$ for the

azimuthal mode propagation [18, 24]. Accordingly we set $k_y = 20$/m; however, for higher mode (m > 1) or larger value of k_y the wavelength would be much smaller than the azimuthal dimension of the channel. For the parameters within this range, we observe that there is usually one root that satisfies the condition for unstable growth of the disturbances. However, in some cases more roots are found, but their growth is too low, showing that these roots are very small perturbations in the system. In order to estimate the growth of the ES wave of observable frequency, we solve Eq. (14) for the complex root of $\omega (\equiv \omega_R - i\gamma)$ and plot γ in Figs. (**2-4**).
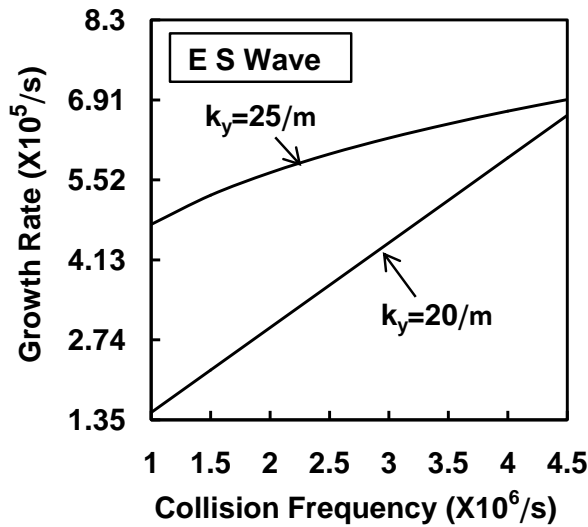
Fig. (2). Variation of growth rate γ of the ES wave with collision frequency for different values of azimuthal wave number in a plasma having Xe ions (M = 131 amu), when $T_e = 10$ eV, $n_0 = 10^{18}$/m^3, $u_0 = 10^6$ m/s and $B_0 = 0.02T$.

Fig. (**2**) shows that the ES wave grows at a faster rate in the presence of larger collision frequency of the electrons. It appears that in the presence of more collisions, the resistive coupling of the oscillations to the electrons' $\vec{E} \times \vec{B}$ drift is stronger and the oscillations grow with higher amplitude. This makes the ES waves to grow faster under the effect of higher collision frequency. It is also seen from the figure that the growth rate is higher for the case of larger wave number. Since larger wave number corresponds to the smaller wavelength oscillations, it is evident that the oscillations of smaller wavelengths are more unstable than the oscillations of larger wavelength. This may also be attributed to the stronger resistive coupling of oscillations to the closed drift of the electrons. In addition, it is observed that the growth rate varies almost linearly with the collision frequency and also increases in direct proportion to the azimuthal wave number. The variation of growth rate with the wave number in the present case is the similar observation as made by Kapulkin *et al.* [24]. Fernandez *et al.* [14] had also observed an enhancement in the growth rate of resistive instability with the collision frequency.

A new feature of the present calculations is the effect of thermal motion of the electrons on the growth of the ES waves. Fig. (**3**) shows the variation of growth rate γ with the electron temperature, where it is observed that the wave grows faster in the presence of larger thermal motion of the electrons. In this case, it is plausible that the resistive coupling of the oscillations be stronger to the electrons' closed drift, resulting in an enhanced growth of the wave. Also it is obtained that the growth gets higher in the plasma of higher density. This is also quite obvious in view of increased collisional effect due to the large density. It would be worth mentioning that the growth of the ES wave in the present case of more realistic plasma with finite T_e is $\sim 10^5$ /s, whereas in a simplified model with the neglect of T_e [13] it was obtained as $\sim 10^6$ Hz. Hence, we can say that these waves grow at a slower rate in a realistic situation.
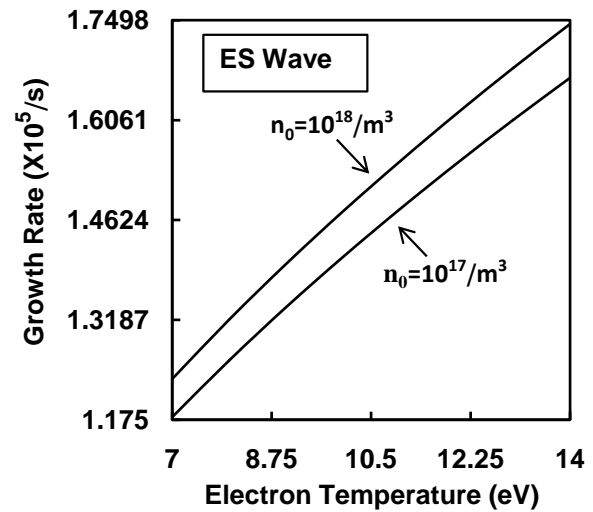
Fig. (3). Variation of growth rate γ of the ES wave with electron temperature for different values of plasma density in a plasma having Xe ions (M = 131 amu), when $v = 10^6$ /s, $k_y = 20$ /m, $u_0 = 10^6$ m/s and $B_0 = 0.02T$.

Finally, in Fig. (**4**) we show the dependence of the growth rate on the electron drift velocity and the magnetic field. Clearly it is observed that the growth of the ES wave is reduced in the presence of larger electron drift velocity. This is plausible, as the resistive coupling of the oscillations to the electrons' drift would be weaker due to the enhanced velocity of the electrons. Moreover, it is evident from the figure that the growth of the ES wave is also suppressed in the presence of stronger magnetic field. The growth is quite sensitive to the change in electron drift velocity and in the presence of stronger magnetic field this sensitivity is enhanced. The reduced growth under the effect of stronger magnetic field is attributed to the weaker coupling of the oscillations to the electrons' closed drift. This happens due to the enhanced gyrofrequency of the electrons and the smaller Larmour radius in the presence of stronger magnetic field.
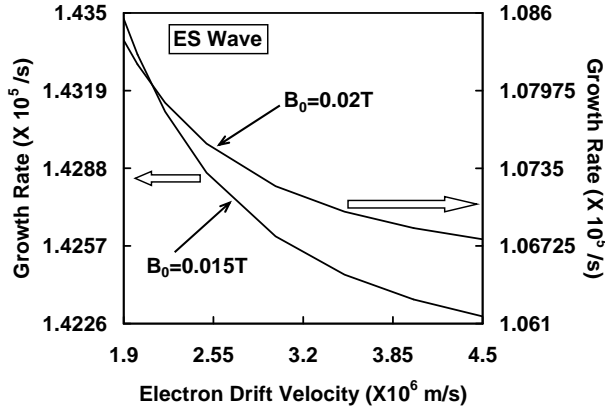
Fig. (4). Weak dependence of growth rate γ of the ES wave on electron drift velocity for different values of magnetic field in a plasma having Xe ions (M = 131amu), when $T_e = 10$ eV, $v = 10^6$ /s, $k_y = 20$ /m and $n_0 = 10^{18}$ /m^3.

4. EM WAVES: DISPERSION EQUATION AND GROWTH RATE

For electromagnetic waves, the linearized equations (5 – 8) are used and the density perturbations are expressed in term of the electric field as

$$n_i = \frac{en_0(k_x E_x + k_y E_y)}{iM(\omega - k_x v_0)^2} \qquad (15)$$

$$n_e = \frac{en_0(\Omega k_x E_y - i\hat{\omega}k_x E_x - i\hat{\omega}k_y E_y - \Omega k_y E_x)}{m\Omega^2(\omega - k_y u_0)F(\omega)} \qquad (16)$$

The x-and y-components of the perturbed current density are obtained as

$$J_x = e\left[n_i v_0 + n_0(v_{ix} - v_{ex})\right] \qquad (17)$$

$$J_y = e\left[-n_e u_0 + n_0(v_{iy} - v_{ey})\right] \qquad (18)$$

From Eqs. (5 – 8) the velocity components are obtained and put in Eqs. (17) and (18). Then, the Maxwell's equations are used in view of the perturbed electric and magnetic fields of the EM wave, and the plasma dielectric tensor ε_{ij} is obtained as $\varepsilon_{ij}E_j = E_j\delta_{ij} + \dfrac{j_i(E_j)}{i\omega\varepsilon_0}$. Finally, the wave equation $\left(k^2\delta_{ij} - k_i k_j - \dfrac{\omega^2}{c^2}\varepsilon_{ij}\right)E_j = 0$ is written in the following form

$$k_x^2\varepsilon_{xx} + k_y k_x(\varepsilon_{xy} + \varepsilon_{yx}) + k_y^2\varepsilon_{yy} - \frac{\omega^2}{c^2}(\varepsilon_{xx}\varepsilon_{yy} - \varepsilon_{xy}\varepsilon_{yx}) = 0 \quad (19)$$

where the components of the dielectric tensor are given by

$$\varepsilon_{xx} = 1 - \frac{\omega_i^2 k_x v_0}{\omega(\omega - k_x v_0)^2} - \frac{\omega_i^2}{\omega(\omega - k_x v_0)}$$
$$+ \frac{(\omega - k_y u_0)\omega_e^2}{\omega\Omega^2} - \frac{\omega_e^2 Y_e T_e(\Omega^2 k_y^2 + \hat{\omega}^2 k_x^2)}{F(\omega)m\omega\Omega^4(\omega - k_y u_0)} \qquad (20)$$

$$\varepsilon_{xy} = \frac{i\omega_e^2}{\omega\Omega} - \frac{\omega_i^2 k_y v_0}{\omega(\omega - k_x v_0)^2} - \frac{\omega_e^2 Y_e T_e(\hat{\omega}k^2 - \Omega k_x k_y)}{m\Omega^3\omega(\omega - k_y u_0)F(\omega)} \qquad (21)$$

$$\varepsilon_{yx} = \frac{i\omega_e^2 Y_e T_e\left[\hat{\omega}(k_x^2 - k_y^2) + i\Omega k_x k_y\right]}{m\Omega^3\omega(\omega - k_y u_0)F(\omega)}$$
$$- \frac{i\omega_e^2}{\omega\Omega} + \frac{\omega_e^2 u_0(\hat{\omega}k_x - i\Omega k_y)}{\Omega^2\omega(\omega - k_y u_0)F(\omega)} \qquad (22)$$

$$\varepsilon_{yy} = 1 + \frac{\omega_e^2 u_0(\hat{\omega}k_y + i\Omega k_x)}{\Omega^2\omega(\omega - k_y u_0)F(\omega)}$$
$$- \frac{\omega_i^2}{\omega(\omega - k_y u_0)}$$
$$- \frac{\omega_e^2 Y_e T_e(\Omega^2 k_x^2 + \hat{\omega}^2 k_y^2)}{m\Omega^4\omega(\omega - k_y u_0)F(\omega)}$$
$$+ \frac{\omega_e^2\hat{\omega}}{\omega\Omega^2} \qquad (23)$$

together with

$$F(\omega) = \left(1 - \frac{Y_e T_e k^2\hat{\omega}}{m\Omega^2(\omega - k_y u_0)}\right) \qquad (24)$$

It is worth noting that under the limit $T_e = 0$, Eqs. (15) and (16) reduce to Eqs. (24) and (27) of Litvak and Fisch [13]. Also the tensor components (20 – 23) reduce to their respective expressions (32 – 35).

As done for the case of ES waves, here also we consider only azimuthal propagation of the waves. So we put $k_x = 0$ and take $k_y = k$ in the wave equation (19) in order to get

$$\frac{k^2 c^2}{\omega^2} = \varepsilon_{xx} - \frac{\varepsilon_{xy}\varepsilon_{yx}}{\varepsilon_{yy}} \qquad (25)$$

After substituting the values of the components of dielectric tensor, we obtain the following dispersion equation for the EM waves

$$B_1\omega^6 + B_2\omega^5 + B_3\omega^4 + B_4\omega^3 + B_5\omega^2 + B_6\omega + B_7 = 0 \qquad (26)$$

where various coefficients are given by

$$B_1 = A_1 c_1 t_6 - c_1^2 A^2\Omega^2$$

$$B_2 = A_1 c_1 t_7 - t_1 t_6 - A\Omega c_4$$

$$B_3 = A_1\Omega^2 k^2 u_0^2 c_1^2 - A\Omega c_5 - A_1 c_1 t_9 - t_1 t_7 + t_2 t_6 - A_1 c_2 t_8$$

$$B_4 = t_1 t_9 + t_2 t_7 + A_1 c_2 t_{10} - A\Omega c_6 - 2Y_e^2 T_e^2\omega_e^4 k^4 v + h_1$$

$$B_5 = h_2 + k^2 c^2\left[\begin{array}{l} c_1^2\Omega^2(2Ak^2 u_0^2 - \omega_i^2) - c_1(A_3 + ku_0 A_2 + 2Ac_2\Omega^2 v) \\ + 2c_2 Y_e T_e\omega_e^2 k^2 v - A_1\Omega^2 c_7 \end{array}\right]$$

$$B_6 = k^2 c^2\left[ku_0(2c_1^2\omega_i^2\Omega^2 + A\Omega^2 c_7 + c_1 A_3) + c_2 v(2Ac_1 ku_0\Omega^2 - c_8)\right] + h_3$$

$$B_7 = \omega_i^2\Omega\left\{\Omega\left[k^2 c^2 c_7 - \omega_i^2(c_2^2 - c_1^2 k^2 u_0^2)\right] + kv_0 c_{10}\right\}$$

together with

$$A = \left(\frac{\omega_e}{\Omega}\right)^2, \quad A_1 = 1 + A, \quad A_2 = c_8 + 2u_0 Y_e T_e \omega_e^2 k^3,$$

$$A_3 = ku_0 c_8 + Y_e T_e \omega_e^2 k^2 (u_0^2 k^2 - v^2),$$

$$c_1 = m\Omega^2 + Y_e T_e k^2, \quad c_2 = v Y_e T_e k^2,$$

$$c_3 = Y_e T_e \omega_e^2 k^2 - c_1 ku_0 A\Omega, \quad c_4 = c_1 k(Y_e T_e \omega_e^2 k - 2u_0 c_1 A\Omega),$$

$$c_5 = Y_e T_e \omega_e^2 k^2 (c_2 + c_1 v - 2ku_0 c_1) + c_1 c_8 - A\Omega c_7,$$

$$c_6 = Y_e T_e \omega_e^2 k^2 \left[c_1 k^2 u_0^2 - vc_2 - ku_0(c_2 + c_1 v) \right] - ku_0 c_1 c_8,$$

$$c_7 = c_1^2 k^2 u_0^2 - c_2^2, \quad c_8 = \omega_e^2 \Omega^2 ku_0 m,$$

$$c_9 = c_2(ku_0 c_1 A\Omega - c_3) - vc_1 Y_e T_e \omega_e^2 k^2,$$

$$c_{10} = u_0 Y_e T_e \omega_e^2 k^3 (vc_1 + c_2) - c_2 c_8,$$

$$h_1 = ku_0 \left[c_1 \omega_i^2 (t_6 + A_1 c_1 \Omega^2) - Ac_2 t_8 \right]$$
$$+ k^2 c^2 c_1 \left\{ A_2 + ku_0 \left[Y_e T_e \omega_e^2 k^2 - \Omega^2 c_1 (A + 2A_1) \right] \right\},$$

$$h_2 = \omega_i^2 \left[c_1 ku_0 t_7 + \Omega^2 (c_2^2 A_1 - c_1 ku_0 t_1) - c_2 t_8 \right]$$
$$- v Y_e T_e \omega_e^2 k^2 (c_8 - 2u_0 Y_e T_e \omega_e^2 k^3)$$
$$- t_2 t_9 - Ac_2 k(2c_1 \Omega^2 \omega_i^2 v_0 + u_0 t_{10}),$$

$$h_3 = \omega_i^2 \left\{ ku_0 \left[\Omega^2 (c_1 t_2 - Ac_2^2) - c_1 t_9 \right] + c_2 t_{10} + \Omega k v_0 c_9 \right\},$$

$$t_1 = (A_1 + A)ku_0 c_1,$$

$$t_2 = c_1(Ak^2 u_0^2 - \omega_i^2) - Y_e T_e \omega_e^2 k^2, \quad t_3 = vAc_1 + A_1 c_2,$$

$$t_4 = c_1(\omega_i^2 - Ak^2 u_0^2) + vAc_2, \quad t_5 = Aku_0(c_2 + c_1 v),$$

$$t_6 = A_1 c_1 \Omega^2 - Y_e T_e \omega_e^2 k^2, \quad t_7 = A_2 - t_1 \Omega^2,$$

$$t_8 = 2v Y_e T_e \omega_e^2 k^2 - t_3 \Omega^2, \quad t_9 = A_3 + t_4 \Omega^2, \quad t_{10} = t_5 \Omega^2 - vc_8$$

We solve numerically the dispersion equation (26) for its complex root $\omega(\equiv \omega_R - i\gamma)$ by giving typical values to the magnetic field, azimuthal wave number, collision frequency, electron drift velocity, ion drift velocity, and electron temperature. The effect of these parameters on the growth γ of the EM wave is studied in Figs. (**5-8**).

Fig. (**5**) shows the effect of magnetic field and the electron drift velocity on the growth rate of the EM wave, when $T_e = 10$ eV, $v = 10^6$ /s, $k_y = 20$ /m, $n_0 = 10^{18}$ /m^3 and $v_0 = 5 \times 10^4$ m/s. It can be seen that the wave grows faster for the larger values of the magnetic field and drift velocity of the electrons. In an experiment, Wei *et al.* [25] had also observed an enhancement in the growth of coupling instability with the magnetic field. In the present case, the reason for the enhanced growth rate can be understood as follows. Since the electrons have their drift in the y-direction, they experience the Lorentz force due to the magnetic field in the negative of x-direction, i.e. in the direction opposite to the ions' drift. As the perpendicular / transverse oscillations are important for the EM waves and – x direction is perpendicular to the wave vector, the larger Lorentz force helps these transverse oscillations to grow.

Hence, the wave grows faster in the presence of stronger magnetic field. Since the drift velocity can be correlated with the discharge voltage, it can be said that the growth rate is increased with the discharge voltage. Esipchuk and Tilinin [26] had also reported the proportionality of the frequency of drift instability to the discharge voltage. The increase in the growth rate may be attributed to the strong coupling between the electric field and electron current [27]. We can also explain this enhanced growth rate based on the magnitude of the Lorentz force acting on the electrons in the opposite direction to the ions' drift. Since the Lorentz force acting in the transverse direction is enhanced in the presence of larger electron drfit, it is obvious that the transverse oscillations will grow more for the case of larger drift.
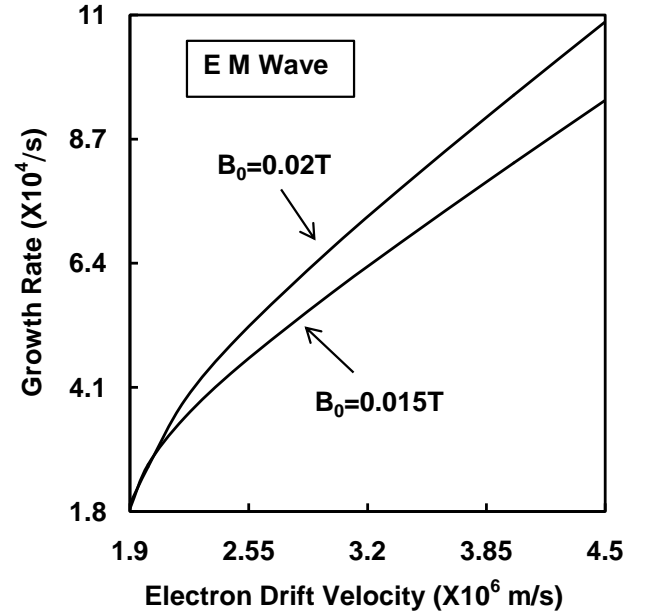
Fig. (5). Variation of growth rate γ of the EM wave with electron drift velocity for different values of magnetic field in a plasma having Xe ions (M = 131amu), when $T_e = 10$ eV, $v = 10^6$ /s, $k_y = 20$ /m, $n_0 = 10^{18}$ /m^3 and $v_0 = 5 \times 10^4$ m/s.

We have plotted Fig. (**6**) for examining the variation of growth rate under the effect of collision frequency and the azimuthal wave number. It is clearly seen that the wave grows at a faster rate in the presence of more electron collisions. Since the stronger resistive coupling of the oscillations to the electrons' closed drift requires the electron collisions, it is obvious that this instability will grow faster in the presence of higher collision frequency. On the other hand, almost parabolic nature of the EM graphs shows that the growth of the EM wave is directly proportional to the square root of the collision frequency. During the simulation studies of resistive instability, Fernandez *et al.* [14] had also observed the growth rate to be directly proportional to the square root of the collision frequency. The dependence of growth rate on the azimuthal wave number reveals that the growth is enhanced for the larger values of the wave number. It means the oscillations of smaller wavelengths are more unstable. Kapulkin *et al.* [25] have also observed the rate of growth of instability to increase in direct proportion to the

azimuthal wave number. On the other hand, in a study of microwave and plasma interaction [28], instabilities have also been found to grow when the frequency of the microwave was brought down to the near cutoff conditions.
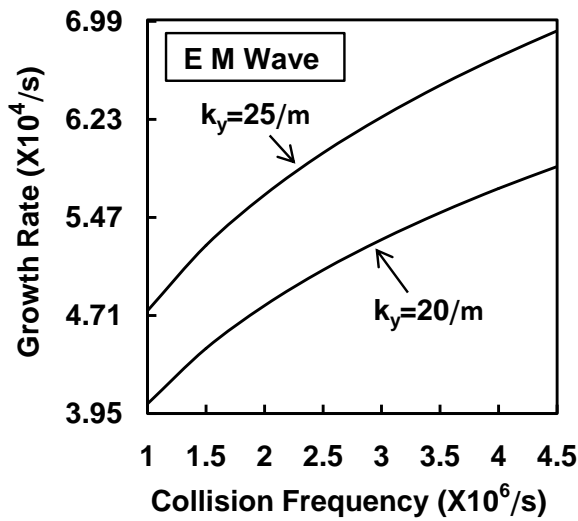
Fig. (6). Variation of growth rate γ of the EM wave with collision frequency for different values of azimuthal wave number in the plasma having Xe ions (M = 131amu), when $T_e = 10$ eV, $n_0 = 10^{18}$ /m³, $B_0 = 0.02T$, $u_0 = 10^6$ m/s and $v_0 = 5 \times 10^4$ m/s.
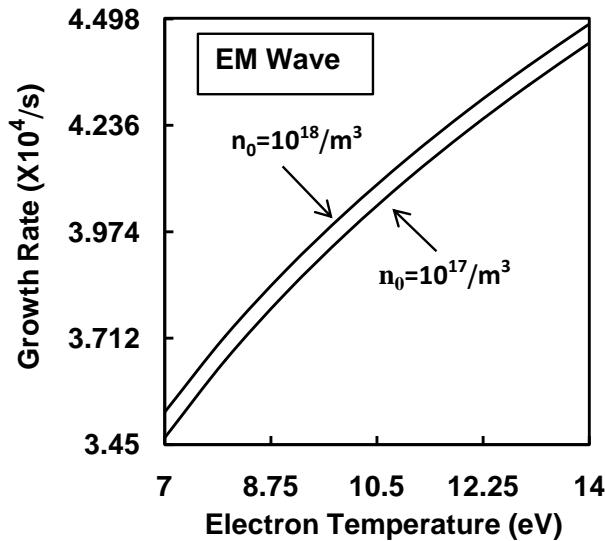
Fig. (7). Dependence of growth rate γ of the EM wave on electron temperature for different values of plasma density in a plasma having Xe ions (M = 131amu), when $v = 10^6$ /s, $k_y = 20$ /m, $B_0 = 0.02T$, $u_0 = 10^6$ m/s and $v_0 = 5 \times 10^4$ m/s.

The dependence of growth rate of the EM wave on the electron temperature and the density is shown in Fig. (**7**), where it is observed that the wave grows faster if the electrons carry higher temperature or their concentration is large. The higher growth rate for the case of higher electron temperature and their large concentration can be explained

based on the probability of the collisions. Since the collision is the requirement for the resistive instability, it is obvious that the wave will grow fast if more collisions take place in the plasma. In fact the same is expected in the case of higher temperature electrons, as the probability of collisions is high in the presence of enhanced thermal motion of the electrons. Moreover, their large density will also enhance the collisional effect. Therefore, higher growth is realized for the higher electron density also. Contrary to this, the opposite effect of ion drift velocity is observed on the growth of the EM wave (Fig. **8**). Actually in the presence of their large drift, the ions try to diminish the transverse oscillations of the electrons in the x-direction. Since the transverse oscillations are important for the growth of the wave, the lower growth rate is realized in the presence of higher drift of the ions.
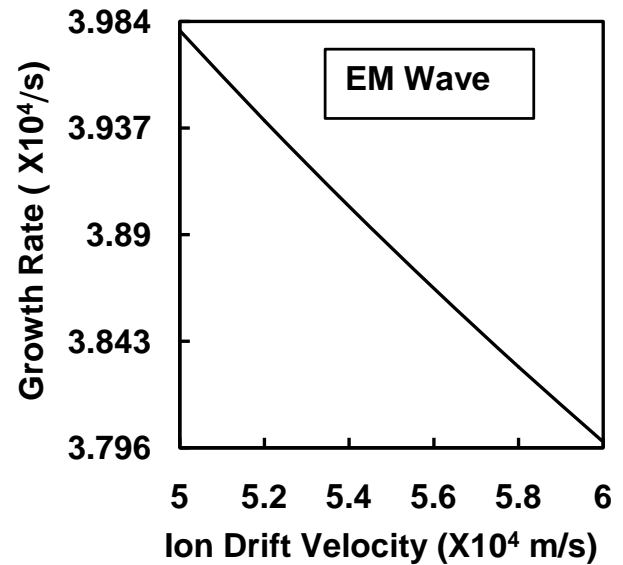
Fig. (8). Variation of growth rate γ of the EM wave with ion drift velocity in a plasma having Xe ions (M = 131amu), when $v = 10^6$ /s, $n_0 = 10^{18}$ /m³, $T_e = 10$ eV, $k_y = 20$ /m, $u_0 = 10^6$ m/s and $B_0 = 0.02T$.

In addition to the above ES and EM instabilities, two nongrowing ES and EM waves are also observed in the present plasma model. The ES wave is found to have velocity $\sim 10^5$ m/s, though the EM wave propagates at slower velocity ($\sim 10^4$ m/s). The ES wave is found to attain larger velocity under the effect of higher plasma density and the magnetic field, and the velocity increases from $2 \cdot 66 \times 10^5$ m/s ($2 \cdot 68 \times 10^5$ m/s) to $2 \cdot 68 \times 10^5$ m/s ($3 \cdot 58 \times 10^5$ m/s) when the plasma density (magnetic field) is enhanced from 10^{17} /m³ ($0 \cdot 015$ T) to 10^{18} /m³ ($0 \cdot 020$ T). On the other hand, the velocity of the EM wave is enhanced with an increment in the plasma density, electron drift velocity, magnetic field and electron temperature, and it is reduced with the collision frequency. The phase velocity is found to increase from $2 \cdot 21 \times 10^4$ m/s to $2 \cdot 53 \times 10^4$ m/s ($6 \cdot 3 \times 10^4$ m/s) when the magnetic field (electron drift velocity) is increased from $0 \cdot 015$ T (1×10^6 m/s) to $0 \cdot 020$ T (5×10^6 m/s), however it decreases to $2 \cdot 19 \times 10^4$

m/s when the collison frequency is enhanced from 1×10^6 /s to 3×10^6 /s. Also the phase velocity attains the value of $2 \cdot 21 \times 10^4$ m/s from $1 \cdot 5 \times 10^4$ m/s ($1 \cdot 96 \times 10^4$ m/s) when the plasma density (electron temperature) is increased from 10^{17} /m^3 (7 eV) to 10^{18} /m^3 (10 eV). It means the phase velocity of the EM wave varies from $1 \cdot 5 \times 10^4$ m/s to $6 \cdot 3 \times 10^4$ m/s for these set of parameters, though the velocity of the ES wave shows a weak dependence and is enhanced from $2 \cdot 66 \times 10^5$ m/s to $3 \cdot 5 \times 10^5$ m/s.

5. CONCLUSIONS

We have derived equations in oscillation frequency ω corresponding to the ES and EM waves propagating in azimuthal direction in a Hall thruster channel, and obtained their solutions numerically. These waves are found to be unstable under the effect of coupling with the electrons' $\vec{E} \times \vec{B}$ drift in the presence of their collisions. Consistent to the observation made by Litvak and Fisch [13], the ES wave grows faster than the EM wave. Nevertheless, the growth rates of these instabilities attain relatively smaller values under more realistic situation. The growth of the ES wave ranges from $1 \cdot 35 \times 10^5$ – $6 \cdot 9 \times 10^5$ /s and that of the EM wave ranges from 1.8×10^4 – 11×10^4/s for the parameters taken in the present study within the prescribed range. The instability corresponding to the ES wave is found to be more crucial.

ACKNOWLEDGEMENT

REFERENCES

[1]   Zhurin VV, Kaufman HR, Robinson RS. Physics of closed drift thrusters. Plasma Sources Sci Technol 1999; 8: R1-20.
[2]   Bouchoule A, Kadlec CP, Prioul M, *et al*. Transient phenomena in closed electron drift plasma thrusters: Insights obtained in a French cooperative program. Plasma Sources Sci Technol 2001; 10: 364-77.
[3]   Adam JC, Boeuf JP, Dubuit N, *et al*. Physics, simulation and diagnostics of Hall effect thrusters. Plasma Phys Control Fusion 2008; 50: 124041 (1-17).
[4]   Bouchoule A, Boeuf JP, Heron A, Duchemin O. Physical investigation and developments of Hall plasma thrusters. Plasma Phys Control Fusion 2004; 46: B407-21.
[5]   Schmidt DP, Meezan NB, Hargus Jr WA, Cappelli MA. A low-power, linear-geometry Hall plasma source with an open electron-drift. Plasma Sources Sci Technol 2000; 9: 68-76.
[6]   Kaufman HR. Technology of closed-drift thrusters. AIAA J 1985; 23: 78-86.
[7]   Choueiri EY. Fundamental difference between the two Hall thruster variants. Phys Plasmas 2001; 8: 5025-33.
[8]   Morozov AI, Esipchuk YV, Tilinin GN, *et al*. Plasma accelerator with closed electron drift and extended acceleration zone. Sov Phys Tech Phys 1972; 17: 38-45.
[9]   Kim V. Main physical feature and processes determining the performance of stationary plasma thrusters. J Prop Power 1998; 14: 736-43.
[10] Zharinov AV, Popov YS. Acceleration of plasma by a closed Hall current. Sov Phys Tech Phys 1967; 12: 208-11.
[11] Garner CE, Brophy JR, Polk JE, *et al*. Experimental evaluation of Russian anode layer thrusters. AIAA J 1994; 94: 3010(1-12).
[12] Choueiri EY. Plasma oscillations in Hall thrusters. Phys Plasmas 2001; 8: 1411-26.
[13] Litvak AA, Fisch NJ. Resistive instabilities in Hall current plasma discharge. Phys Plasmas 2001; 8: 648-51.
[14] Fernandez E, Scharfe MK, Thomas CA, *et al*. Growth of resistive instabilities in $\vec{E} \times \vec{B}$ plasma discharge simulations. Phys Plasmas 2008; 15: 012102 (1-10).
[15] Keidar M. Anodic plasma in Hall thrusters. J Appl Phys 2008; 103: 053309 (1-5).
[16] Keidar M, Beilis II. Sheath and boundary conditions for plasma simulations of a Hall thruster discharge with magnetic lenses. Appl Phys Lett 2009; 94: 191501 (1-3).
[17] Keidar M, Boyd ID. Effect of a magnetic field on the plasma plume from Hall thrusters. J Appl Phys 1999; 86: 4786-91.
[18] Litvak AA, Fisch NJ. Rayleigh instability in Hall thrusters. Phys Plasmas 2004; 11: 1379-82.
[19] Ducrocq A, Adam JC, Heron A, Laval G. High-frequency electron drift instability in the cross-field configuration of Hall thrusters. Phys Plasmas 2006; 13: 102111 (1-8).
[20] Barral S, Ahedo E. Low-frequency model of breathing oscillations in Hall discharges. Phys Rev E 2009; 79: 046401 (1-11).
[21] Boeuf JP, Garrigues LJ. Low frequency oscillations in a stationary plasma thruster. J Appl Phys 1998; 84: 3541-54.
[22] Chesta E, Meezan NB, Cappelli MA. Stability of a magnetized Hall plasma discharge. J Appl Phys 2001; 89: 3099-07.
[23] Smirnov A, Raitses Y, Fisch NJ. Plasma measurements in a 100W cylindrical Hall thruster. J Appl Phys 2004; 95: 2283-92.
[24] Kapulkin A, Kogan A, Guelman M. Noncontact emergency diagnostics of SPT in flight. Acta Astronautica 2004; 55: 109-19.
[25] Wei L, Jiang B, Wang C, *et al*. Characterization of coupling oscillation in Hall thrusters. Plasma Sources Sci Technol 2009; 18: 045020 (1-6).
[26] Esipchuck YV, Tilinin GN. Drift instability in a Hall-current plasma accelerator. Sov Phys Tech Phys 1976; 21: 417-23.
[27] Chable S, Rogier F. Numerical investigation and modeling of stationary plasma thruster low frequency oscillations. Phys Plasmas 2005; 12: 033504 (1-9).
[28] Aria AK, Malik HK. Wakefield field generation in a plasma filled rectangular waveguide. The Open Plasma Phys J 2008; 1: 1-8.